ARTICLE

Reactions of [(dmpe)$_2$MnH(C$_2$H$_4$)]: Synthesis and Characterization of Manganese(I) Borohydride and Hydride Complexes

Received 00th January 20xx,
Accepted 00th January 20xx

DOI: 10.1039/x0xx00000x

Jeffrey S. Price,[a] Declan M. DeJordy,[a] David J. H. Emslie,*[a] and James F. Britten[b]

Reactions of *trans*-[(dmpe)$_2$MnH(C$_2$H$_4$)] (**1**) with BH$_3$(NMe$_3$), 9-BBN, and HBMes$_2$ yielded the manganese(I) borohydride complexes [(dmpe)$_2$Mn(μ-H)$_2$BR$_2$] (**3**: R = H, **4**: R$_2$ = C$_8$H$_{14}$, **5**: R = Mes). The reaction of **1** with BH$_3$(NMe$_3$) proceeds via ethylene substitution. By contrast, a detuerium labelling study indicates that the reaction of **1** with HBMes$_2$ involves initial isomerization of **1** to an unobserved 5-coordinate ethyl intermediate, [(dmpe)$_2$MnEt], which reacts with the hydroborane to afford EtBR$_2$ and [(dmpe)$_2$MnH], followed by reaction with a second equivalent of hydroborane to generate **5** (an analogous pathway is likely followed for other base-free hydroboranes such as 9-BBN). Identification of **3-5** as κ^2-borohydride complexes, as opposed to boryl dihydride or hydroborane hydride isomers, is supported by ^{11}B NMR spectroscopy, X-ray diffraction, and Atoms in Molecules calculations. Two byproducts were observed in the syntheses of **3-5**: [{(dmpe)$_2$MnH}$_2$(μ-dmpe)] (**6**) and [(dmpe)$_2$MnH(κ^1-dmpe)] (**7**). These complexes were independently prepared by exposure of **1** to free dmpe under an atmosphere of Ar or H$_2$, and the generality of this synthetic route was demonstrated by the reaction of **1** with PMe$_3$ (under H$_2$) to form [(dmpe)$_2$MnH(PMe$_3$)] (**8**). Complexes **6-8** can exist as isomers with either a *trans* or a *cis* relationship between the hydride and κ^1-coordinated phosphine ligands on manganese. *Trans* to *cis* isomerization of **6-8** is photochemically induced, whereas the reverse reaction occurs under thermal conditions. X-ray crystal structures were obtained for **3-5**, ***trans,trans*-6**, ***cis,cis*-6**, ***trans*-7**, and ***trans*-8**.

Introduction

Our group has previously reported reactions of the ethylene hydride complex *trans*-[(dmpe)$_2$MnH(C$_2$H$_4$)] (**1**)[1,2] with dihydrogen and various hydrosilanes; Scheme 1. Exposure of **1** to H$_2$ formed the previously reported dihydrogen hydride complex [(dmpe)$_2$MnH(H$_2$)] (**2**),[2] while reactions of **1** with primary hydrosilanes afforded the disilyl hydride complexes [(dmpe)$_2$MnH(SiH$_2$R)$_2$] (R = Ph, ^{n}Bu).[3] By contrast, reactions of **1** with secondary hydrosilanes afforded silylene hydride complexes [(dmpe)$_2$MnH(=SiR$_2$)] (R = Ph R = Et), in combination with (in the case of the reaction of **1** with H$_2$SiPh$_2$) the silyl dihydride complex [(dmpe)$_2$MnH$_2$(SiHPh$_2$)].[4] Using DFT calculations and trapping experiments, it was determined that these reactions proceed via initial isomerization of **1** to a 5-coordinate ethyl species [(dmpe)$_2$MnEt] (**A**), as shown in Scheme 1.

Given the diverse reactivity of **1** with hydrosilanes, we were motivated to investigate the reactivity of **1** with hydroboranes. Reactions of transition metal hydride complexes with hydroboranes have been reported to form structures with various boron-containing ligands and bonding

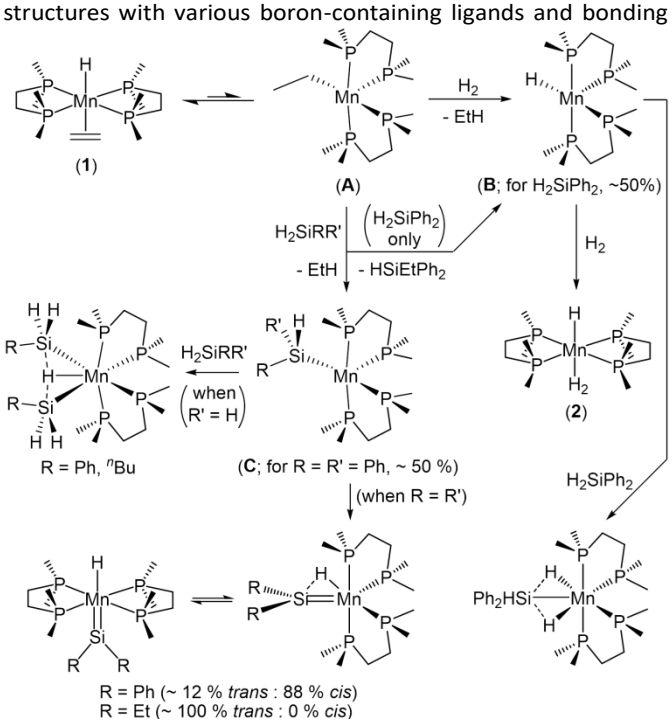

Scheme 1 Reactions of [(dmpe)$_2$MnH(C$_2$H$_4$)] (**1**) with H$_2$ and hydrosilanes to generate dihydrogen hydride (**2**), disilyl hydride, silylene hydride, and silyl dihydride complexes.

[a] *Department of Chemistry, McMaster University, 1280 Main Street West, Hamilton, Ontario, L8S 4M1. E-mail: emslied@mcmaster.ca*
[b] *McMaster Analytical X-ray Diffraction Facility (MAX), McMaster University, 1280 Main Street West, Hamilton, Ontario, L8S 4M1.*

Electronic Supplementary Information (ESI) available: Computational methods, and results, tables of crystal data/crystal structure refinement, and selected NMR spectra (PDF). Cartesian coordinates for the calculated structures (XYZ). CCDC 2002778-2002784. For ESI and crystallographic data in CIF or other electronic format see DOI: 10.1039/x0xx00000x

A-C are proposed intermediates, and only one isomer is shown for all species (except silylene hydride complexes).[3,4]

motifs.[5,6] These include monodentate[7,8] or bidentate[7,9–14] borohydride complexes (a single anionic ligand with either one or two hydrogen atoms bridging between boron and the metal; i and ii in Figure 1), boryl dihydride complexes (containing three anionic ligands; iii in Figure 1),[9,15,16] and hydroborane hydride complexes (featuring anionic hydride and neutral σ-hydroborane ligands; iv in Figure 1).[10,12,16,17] Of these, borohydride complexes are commonly favoured (over hydroborane hydride complexes) in reactions involving substantially Lewis acidic boron centres, and boryl dihydride complexes are favoured in reactions with electron-rich metal centres with an accessible oxidation state 2 units higher.[13,18] Complexes with structures intermediate between the bidentate borohydride and boryl dihydride extremes have also been reported,[19,20] and described in various manners including as stretched η^3-hydridoborate *σ*-complexes, or as boryl dihydride complexes with B–H interligand interactions. Additionally, equilibria between various of these isomers have been reported.[9,10,18]

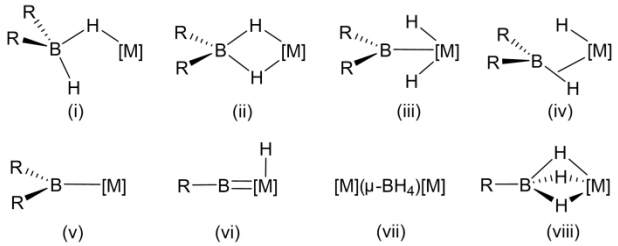

Figure 1 Products observed upon reaction of hydroboranes with transition metal hydride complexes (in the case of borylene or hydride-free boryl complexes, after H_2 elimination): i) monodentate borohydride, ii) bidentate borohydride, iii) boryl dihydride, iv) hydroborane hydride, v) boryl, vi) borylene hydride, vii) bridging borohydride, and viii) tridentate borohydride complexes (the latter are normally prepared via reactions with hydroborate salts).

In addition, reactions of metal hydride complexes with hydroboranes have in some cases been observed to eliminate H_2 to afford boryl (v in Figure 1)[21] or borylene hydride (vi in Figure 1)[14,22] complexes. Furthermore, structures featuring borohydride moieties bridging between multiple metal centres (vii in Figure 1),[23] and tridentate borohydride ligands (viii in Figure 1) have been reported, though the latter are generally prepared via reactions with hydroborate salts.[6]

In the chemistry of manganese(I), complexes incorporating borohydride ligands which are not part of a chelating ligand framework are scarce; the only crystallographically characterized examples are a pair of dimetallic μ-(BH_4) species reported by Riera in the early 1990s (a and b in Figure 2),[24] monometallic complexes reported independently in 2017 by the Figueroa[25] and Gauvin[26] groups with bi- or mono-dentate borohydride ligands (c and d, respectively, in Figure 2), and a monometallic species reported by Ghosh et al. in 2020 featuring a ligand which could be considered a κ^3-borohydride with a terminal phosphine-stabilized boryl substituent (e in Figure 2).[27]

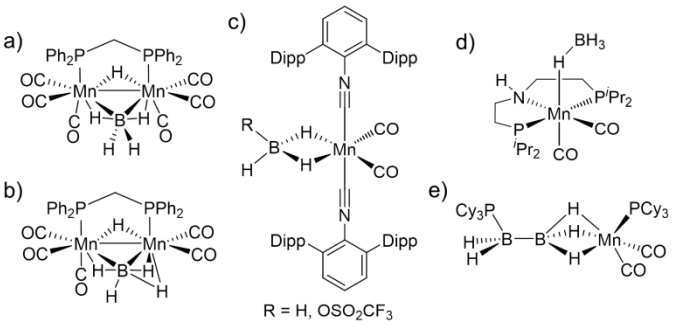

Figure 2 Crystallographically characterized manganese(I) complexes incorporating borohydride ligands which are not part of a chelating ligand framework.

Herein, we discuss the synthesis and characterization of a series of manganese(I) borohydride complexes prepared via reactions of *trans*-[(dmpe)$_2$MnH(C_2H_4)] (**1**) with $BH_3(NMe_3)$, 9-BBN and $HBMes_2$. Furthermore, we identify byproducts observed in the syntheses of these borohydride complexes as pentaphosphine manganese(I) hydride complexes, and demonstrate that such complexes can be prepared directly from **1** by exposure to free phosphines under an atmosphere of argon or dihydrogen.

Results and Discussion

Reaction of [(dmpe)$_2$MnH(C_2H_4)] (**1**)[1,2] with $BH_3(NMe_3)$ at 90 °C afforded the borohydride complex [(dmpe)$_2$Mn(μ-H)$_2$$BH_2$] (**3**) as a purple solid, accompanied by ethylene and free NMe_3 byproducts (Scheme 2; top). In contrast to previously reported reactions of **1** with hydrosilanes, all of which proceed via isomerization of **1** to a 5-coordinate ethyl intermediate (**A**; *vide supra*) with ensuing reactivity to eliminate ethane or an ethylhydrosilane byproduct, this reaction involves ethylene elimination. Whereas the previously reported aluminium analogue of **3**, [(dmpe)$_2$Mn(μ-H)$_2$AlH(μ-H)$_2$AlH(μ-H)$_2$Mn(dmpe)$_2$],[1,2] is a dimer with 5-coordinate aluminium centres, compound **3** is monometallic due to the typical reluctance of boron to adopt a coordination number greater than four. As a consequence, **3** is relatively volatile, subliming at 80 °C at 5 mTorr.

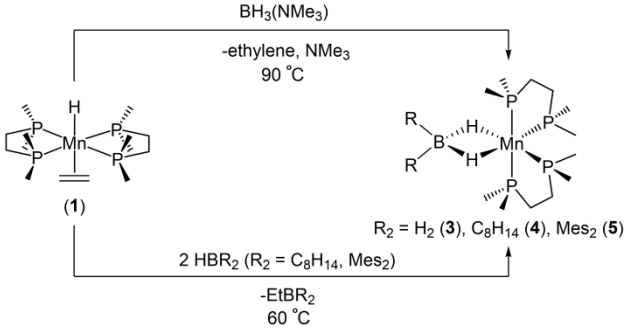

Scheme 2 Reactions of [(dmpe)$_2$MnH(C_2H_4)] (**1**) with hydroboranes to generate borohydride complexes [(dmpe)$_2$Mn(μ-H)$_2$$BR_2$] ($R_2$ = H_2 (**3**), C_8H_{14} (**4**); Mes_2 (**5**)).

Reactions of [(dmpe)$_2$MnH(C_2H_4)] (**1**) with two equivalents of the dialkyl or diaryl hydroboranes, 9-

borabicyclo(3.3.1)nonane (9-BBN; HBC_8H_{14}) or dimesitylborane ($HBMes_2$), at 60 °C yielded isostructural borohydride complexes $[(dmpe)_2Mn(\mu\text{-}H)_2BR_2]$ ($R_2 = C_8H_{14}$ (**4**); R = Mes (**5**)), with $EtBR_2$ as the only spectroscopically observed byproduct (Scheme 2; bottom).‡ While **4** could only be obtained in high purity by manual separation of crystals, **5** was isolated as an analytically pure purple solid. A closely related rhenium(I) tetraphosphino borohydride complex [{*rac*-κ^4-$Ph_2PCH_2CH_2P(Ph)CH_2CH_2P(Ph)CH_2CH_2PPh_2$}$Re(\mu\text{-}H)_2BEt_2$] was reported by Morris et al. in 1993.[28]

The reactions to form **4** and **5** could proceed via two potential pathways (Scheme 3): (a) ethylene substitution, followed by hydroboration of released ethylene by a second equivalent of HBR_2,§ or (b) initial isomerization of **1** to form $[(dmpe)_2MnEt]$ (**A**), followed by reaction with one equivalent of HBR_2 (via oxidative addition and subsequent C–B bond forming reductive elimination, or σ-bond metathesis) to generate $EtBR_2$ and $[(dmpe)_2MnH]$ (**B**), which then reacts with a second equivalent of hydroborane. The former pathway is analogous to that for the reaction of **1** with $BH_3(NMe_3)$, whereas the latter mirrors the reactions of **1** with H_2 and hydrosilanes (*vide supra*).[3,4]

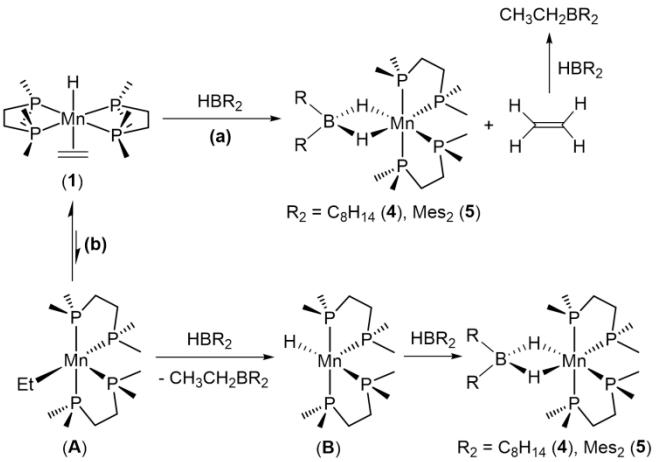

Scheme 3 Potential pathways (a and b) for reactions of HBR_2 ($R_2 = C_8H_{14}$, Mes_2) with $[(dmpe)_2MnH(C_2H_4)]$ (**1**) to form manganese(I) borohydride complexes $[(dmpe)_2Mn(\mu\text{-}H)_2BR_2]$ ($R_2 = C_8H_{15}$ (**4**), Mes_2 (**5**)). **A** and **B** are proposed intermediates.

To distinguish between these possibilities, **1** was exposed to two equivalents of $DBMes_2$ in C_6D_6, exclusively yielding $Mes_2BCH_2CH_3$ and $[(dmpe)_2Mn(\mu\text{-}D)_2BMes_2]$ (***d*₂-5**). This deuterium distribution is consistent with pathway b in Scheme 3, and the same pathway is likely followed in the reaction of **1** with other base-free hydroboranes, such as 9-BBN. The different mechanisms followed in the reactions of **1** with $BH_3(NMe_3)$ versus $HBMes_2$ (and likely 9-BBN) may suggest that the former reaction involves the intact adduct, rather than free borane generated by NMe_3 dissociation.¶

Room temperature NMR spectra of borohydride complexes **3-5** feature two ^{31}P NMR signals (62.6-88.6 ppm) consistent with a disphenoidal arrangement of the phosphorus donors at manganese, and a single low frequency ^1H NMR $Mn(\mu\text{-}\underline{H})_2BR_2$ environment (**3**: –16.5 ppm, **4**: –15.6 ppm, **5**: –14.0 ppm). These signals are significantly broadened, but sharpen upon ^{11}B decoupling. Complexes **3-5** feature a single ^{11}B NMR environment (**3**: 25.3 ppm, **4**: 43.2 ppm, **5**: 27.5 ppm) within the range associated with κ^2-borohydride complexes.[9,29] This is in contrast to boryl[30] or σ-hydroborane[31] complexes, for which the ^{11}B NMR signal is typically shifted to high frequency relative to that of the corresponding free hydroborane monomer. The higher frequency ^{11}B NMR chemical shift for **4** versus **3** and **5** is also consistent with reported trends: (a) free monomeric hydroboranes with alkyl substituents typically have higher ^{11}B NMR chemical shifts than those with aromatic substituents (e.g. 79-82 ppm for $HB(CMe_2CMe_2H)_2$, $HBCy^tBu$, and *B*-H-10-trimethylsilyl-9-borabycyclo[3.3.2]decane,[32] versus 60-74 ppm for $HBMes_2$, $HB(C_6H_2{}^iPr_3\text{-}2,4,6)_2$, $HB(C_6F_5)_2$, and $HBEind_2$, where Eind = 1,1,3,3,5,5,7,7,-octaethyl-*s*-hydrindacen-4-yl),[33] and (b) in $[(OC)_n(Me_3P)_{4-n}Re(\mu\text{-}H)_2BR_2]$ (n = 1 or 2, $R_2 = H_2$ or C_8H_{14}), the ^{11}B NMR chemical shifts for the $H_2B(C_8H_{14})$ complexes are 22-23 ppm higher frequency than those for the BH_4 complexes with identical co-ligands.[7]

For $[(dmpe)_2Mn(\mu\text{-}H)_2BH_2]$ (**3**), the terminal $Mn(\mu\text{-}H)_2B\underline{H}_2$ signal was located at 5.1 ppm in the ^1H NMR spectrum. EXSY NMR spectroscopy did not provide evidence for chemical exchange between the bridging and terminal borohydride environments in **3** up to 339 K. This behaviour contrasts that of the majority of tetrahydroborate transition metal complexes (including the manganese(I) complex reported by the Figueroa group; c in Figure 2),[25] in which the bridging and terminal environments rapidly exchange on the NMR timescale,[6] although analogous behaviour has been observed for rhenium(I) κ^2-borohydide complexes.[7,34] On a longer timescale, exposure of **3** to D_2 (initial pressure of 1.7 atm) for 12 h at 90 °C led to 40 % deuterium incorporation into both the $Mn(\mu\text{-}\underline{H})_2BH_2$ and $Mn(\mu\text{-}H)_2B\underline{H}_2$ environments, accompanied by the formation of HD and H_2. This reactivity may proceed via initial BH_3 dissociation to afford a 5-coordinate hydride intermediate, providing a means to exchange bridging and terminal BH_4 atoms, and allowing for deuterium incorporation in both sites. An alternative mechanism involving isomerization to a boryl dihydrogen complex followed by H_2/D_2 exchange seems less likely given that HD is formed in substantially greater quantities than H_2 (~8:1).

Variable temperature (174-339 K) ^1H NMR spectroscopy of $[(dmpe)_2Mn(\mu\text{-}H)_2BH_2]$ (**3**) shows that both the $Mn(\mu\text{-}\underline{H})_2BH_2$ and $Mn(\mu\text{-}H)_2B\underline{H}_2$ signals transform from relatively sharp singlets at low temperature to multiplets tending towards the expected 1:1:1:1 quartet at high temperature (Figure 3), due to coupling to ^{11}B (I = 3/2, abundance = 80 %, Q = 4.1×10^{-30} m^2; ^{10}B satellites were not resolved, but could contribute the broadness of the signals).[35] The loss of coupling at low temperature (quadrupolar collapse) is caused by faster ^{11}B quadrupolar relaxation as a consequence of longer rotational correlation times (τ_c).[l,36]

X-ray crystal structures were obtained for borohydride complexes **3-5** (Figure 4), and feature an octahedral environment at Mn composed of the two dmpe ligands (with a disphenoidal arrangement of the phosphorus donors) and an κ^2-borohydride ligand (with H atoms on boron located from the difference map). The $Mn(\mu\text{-}H)_2B$ moieties form a near-

perfect plane {the angles between the H(1)–Mn–H(2) and H(1)–B–H(2) planes range from 0.2-8.3° (DFT calcd. 0.0-0.5°)}, and proceeding from **3** to **5**, the Mn–B distances increase from 2.170(4) to 2.206(2) and 2.245(3) Å, likely due to increasing steric hindrance. To our knowledge, **5** is the first crystallographically characterized example of a borohydride complex with two mesityl substituents on boron. Additionally, **4-5** are the first crystallographically characterized manganese borohydride complexes where boron has two terminal hydrocarbyl substituents.

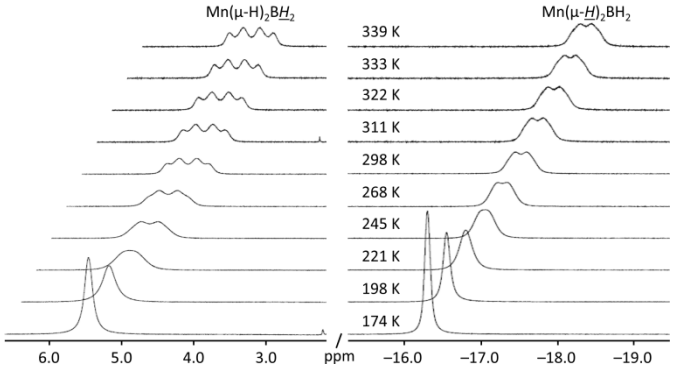

Figure 3 Regions of the ^{1}H NMR spectra of [(dmpe)$_2$Mn(μ-H)$_2$BH$_2$] (**3**) containing the terminal Mn(μ-H)$_2$B*H*$_2$ (left) and bridging Mn(μ-*H*)$_2$BH$_2$ (right) signals from 174-339 K, showing quadrupolar collapse at low temperature (500 MHz, d_8-toluene). The x-axis corresponds to the bottom spectrum, and for clarity, all other spectra are shifted 0.2 ppm to the right (lower frequency) relative to the spectrum below. Spectra on the left-hand side are truncated at 6.5 ppm to remove signals from d_7-toluene.

Description of **3-5** as borohydride complexes, as opposed to boryl dihydride or hydroborane hydride isomers (Figure 1; *vide supra*), is supported by acute H(1)–Mn–H(2) angles[9] of 65(2)-75(2)°, short Mn–H (1.66(3)-1.78(4) Å) and B–(μ-H) (1.19(4)-1.34(4) Å) distances, and Mn–H(1) and B–H(1) distances that are statistically equivalent to Mn–H(2) and B–H(2), respectively. Additionally, the Mn–B distances of 2.170(4)-2.245(3) Å are longer than expected for a boryl complex; the majority of hydride-free, manganese complexes containing a monodentate boryl ligand feature Mn–B distances ranging from 2.02-2.11 Å,[37] though a pair of boryl complexes with extremely bulky B(NDippCH)$_2$ groups have similar Mn–B distances of 2.178(2)-2.229(3) Å.[38] The Mn–B distances in **3-5** are also comparable to those in Figueroa's[25] manganese(I) κ^2-borohydride complexes (c in Figure 2; 2.142(7)-2.166(6) Å).[††] Furthermore, the angle between Mn, B, and the centroid between the two atoms terminally coordinated to boron is approximately 180°, which is inconsistent with a hydroborane hydride complex.[‡‡]

DFT calculations (ADF, gas phase, all-electron, PBE, D3-BJ, TZ2P, ZORA) were employed to further corroborate the assignment of complexes **3-5** as κ^2-borohydride species. In each case, geometry optimized structures feature B–(μ-H) distances within a narrow range (1.32-1.34 Å), a B–(μ-H) Mayer bond order of 0.44-0.55, and Mn–(μ-H) and Mn–B Mayer bond orders of 0.45-0.54 and 0.35-0.43, respectively (Table S1). Atoms in Molecules (AIM) calculations[39] afforded B–(μ-H) and Mn–(μ-H) bond critical points (bcps), but did not locate a bcp between Mn and B (shown for **3** in Figure 5),[20] indicating that any contribution from a boryl dihydride resonance structure is limited. For the two B–(μ-H) or two Mn–(μ-H) bcps in each complex, the various density properties {electron density (ρ), Laplacian of the electron density (∇^{2}ρ), ellipticity (ε), and energy components (G, V, and H)} are nearly identical (Table S1), which is inconsistent with a hydroborane hydride structure. Despite the lack of Mn–B AIM bond path, the bond delocalization index (δ) indicates substantial electron density shared between Mn and B (0.188-0.230), consistent with Mn–borohydride bonding involving the B–H σ-bonds. In addition, the ring critical point (rcp) in the centre of the Mn(μ-H)$_2$B unit lies along the Mn–B axis, and the Mn–(μ-H), and to a lesser extent B–(μ-H), bond paths are curved in the direction of the rcp. Consequently, the Mn–(μ-H) bond paths are 0.07-0.12 Å longer than the corresponding Mn–H distances in **3-5**.

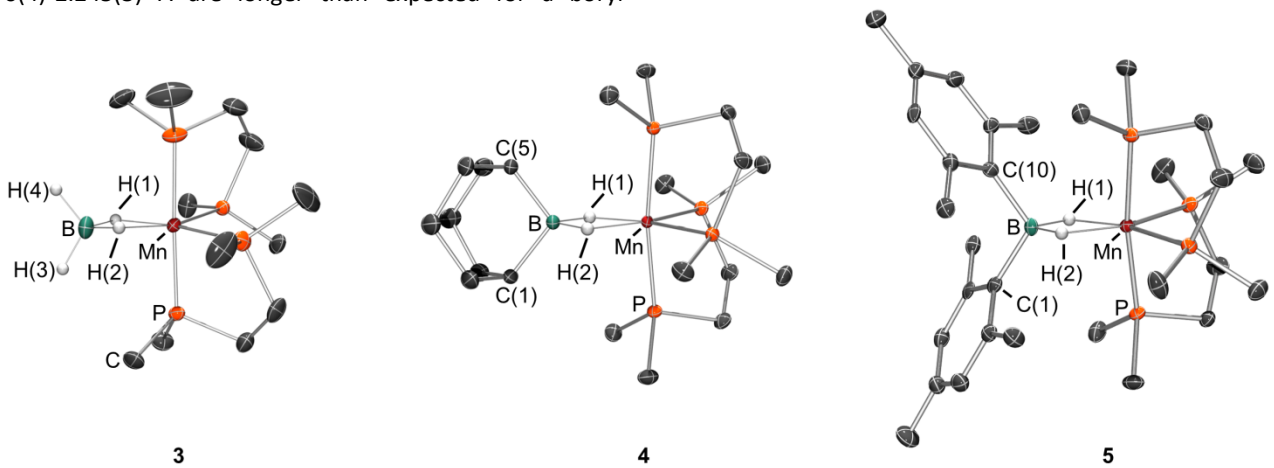

Figure 4 X-ray crystal structures of [(dmpe)$_2$Mn(μ-H)$_2$BH$_2$] (**3**, left), [(dmpe)$_2$Mn(μ-H)$_2$BC$_8$H$_{14}$] (**4**, middle), and [(dmpe)$_2$Mn(μ-H)$_2$BMes$_2$] (**5**, right), with ellipsoids at 50 % probability. Most hydrogen atoms have been omitted for clarity. Hydrogen atoms on Mn and B were located from the difference map and refined isotropically. For **3**, distances (Å) and angles (deg): Mn–B 2.170(4), Mn–H(1) 1.76(4), Mn–H(2) 1.78(4), B–H(1) 1.34(4), B–H(2) 1.31(4), B–H(3) 1.19(5), B–H(4) 1.18(4), H(1)–Mn–H(2) 75(2), H(1)–B–H(2) 109(2), Mn–B–centroid{H(3), H(4)} 173.6, ∠{H(1)–Mn–H(2) plane to H(1)–B–H(2) plane} 8.3. For **4**, distances (Å) and angles (deg): Mn–B 2.206(2), Mn–H(1) 1.71(2), Mn–H(2) 1.66(3), B–H(1) 1.31(2), B–H(2) 1.25(2), B–C(1) 1.624(2), B–C(5) 1.626(3), H(1)–Mn–H(2) 70(1), H(1)–B–H(2) 99(1), Mn–B–centroid{C(1), C(5)} 178.7, ∠{H(1)–Mn–H(2) plane to H(1)–B–H(2) plane} 3.5. For **5**, distances (Å) and angles (deg): Mn–B 2.245(3), Mn–H(1) 1.69(4), Mn–H(2) 1.72(4), B–H(1) 1.24(3), B–H(2) 1.19(4), B–C(1) 1.647(5), B–C(10) 1.647(6), H(1)–Mn–H(2) 65(2), H(1)–B–H(2) 97(2), Mn–B–centroid{C(1), C(10)} 179.4, ∠{H(1)–Mn–H(2) plane to H(1)–B–H(2) plane} 0.2.

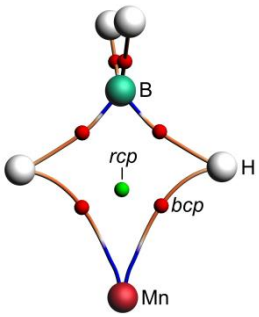

Figure 5. The 'Mn(μ-H)$_2$BH$_2$' core of the DFT calculated structure of [(dmpe)$_2$Mn(μ-H)$_2$BH$_2$] (**3**) showing Atoms in Molecules (AIM) bond paths between displayed atoms, associated bond critical points (bcps; small red spheres), and a ring critical point (rcp; small green sphere). Phosphine ligands (along with associated bond paths, bcps, and rcps) have been removed for clarity. Analogous results were observed for borohydride complexes **4** and **5**.

In the syntheses of **3**-**5**, ^{1}H NMR spectra of the crude reaction mixtures contained two nearly overlapping MnH signals at –15.74 and –15.72 ppm, which were subsequently assigned to [{(dmpe)$_2$MnH}$_2$(μ-dmpe)] (**6**) and [(dmpe)$_2$MnH(κ^1-dmpe)] (**7**); *vide infra*. The additional dmpe ligand (0.5 or 1 equiv. per Mn) in these complexes must be generated by decomposition of one or more reaction product or intermediate.

The same mixture of hydride complexes (**6** and **7**) was independently prepared by the reaction of [(dmpe)$_2$MnH(C$_2$H$_4$)] (**1**) with free dmpe under argon (overnight at 105 °C), or more cleanly under H$_2$ (several days at 60 °C) (Scheme 4). The formation of bimetallic **6** is favoured using an approximate 1:2 ratio of dmpe to **1**, whereas monometallic **7** is favoured using a 3:2 ratio. The syntheses of **6** and **7** under argon proceed via ethylene substitution, whereas those under H$_2$ involve initial reaction of **1** with one equiv. of H$_2$ to generate [(dmpe)$_2$MnH] (**B**) and ethane. Intermediate **B** can coordinate to a free phosphine donor to form **6** or **7**, or a second equivalent of H$_2$ to generate [(dmpe)$_2$MnH(H$_2$)] (**2**; observed by NMR spectroscopy during the course of the reaction). Compound **2** then converts to **6** or **7** by phosphine substitution of the H$_2$ ligand (Jones et al. have shown that the H$_2$ ligand in **2** can undergo dissociative substitution with a range of neutral donors; CO, isonitriles, ethylene, and N$_2$).[40]

Washing the crude mixture of **6** and **7** with hexanes left behind less-soluble dimetallic [{(dmpe)$_2$MnH}$_2$(μ-dmpe)] (**6**), which was isolated as a yellow powder. In contrast, monometallic [(dmpe)$_2$MnH(κ^1-dmpe)] (**7**) was isolated as a yellow powder from the reaction mixture by sublimation at 100 °C (5 mTorr). In solution, **6** and **7** exist as a high (apparent C_{2v}) symmetry and a low (C_1) symmetry isomer, with the relative concentration of the low symmetry isomer increasing from <5 % upon initial isolation to become the dominant species in solution after several weeks in the light at room temperature (this isomerization did not occur in the dark). However, appreciable decomposition of **6** (to form **7**) or **7** (to form **6**), as well as minor (~5 %) decomposition to unidentified hydride-containing species, was also observed over the extended time period of these experiments. Heating solutions containing primarily the low-symmetry isomers of **6** and **7** for a few hours at 90 °C resulted in nearly complete conversion back to the high symmetry isomers.

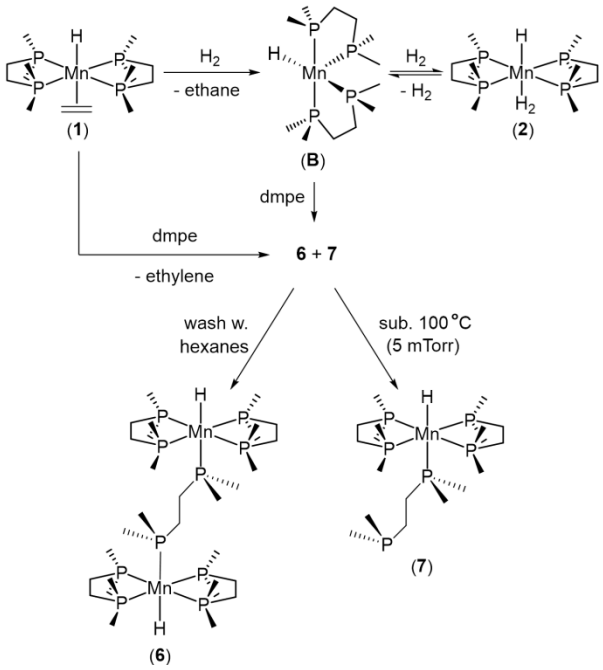

Scheme 4 Reactions of [(dmpe)$_2$MnH(C$_2$H$_4$)] (**1**) with free dmpe to generate phosphine hydride complexes [{(dmpe)$_2$MnH}$_2$(μ-dmpe)] (**6**) and [(dmpe)$_2$MnH(κ^1-dmpe)] (**7**). Only one isomer is shown for **B**, **6**, and **7**.

The high symmetry isomers of **6** and **7** feature an Mn*H* ^{1}H NMR signal at –15.7 ppm, which is a quintet ($^2J_{H,P}$ = 49 Hz) of doublets ($^2J_{H,P}$ = 13 Hz) due to coupling to four *cis* phosphine groups (2 dmpe ligands in a square plane) and one *trans*-disposed μ-dmpe (in **6**) or terminal κ^1-dmpe (in **7**) ligand. The high symmetry isomer of **6**, *trans*,*trans*-[{(dmpe)$_2$MnH}$_2$(μ-dmpe)] (***trans*,*trans*-6**), contains 2.5 equivalents of dmpe per Mn*H* environment, and features two broad singlets at 78.8 and 26.4 ppm in the ^{31}P{^{1}H} NMR spectrum; one for the chelating dmpe ligands, and one for the bridging dmpe ligand. By contrast, the high symmetry isomer of **7**, *trans*-[(dmpe)$_2$MnH(κ^1-dmpe)] (***trans*-7**), contains 3 equivalents of dmpe per Mn*H* environment, and exhibits two broad singlets (at 78.6 and 27.7 ppm) in the ^{31}P{^{1}H} NMR spectrum, accompanied by a sharp doublet (–49.6 ppm, $J_{P,P}$ = 14 Hz) for the pendant phosphine of the κ^1-dmpe ligand (cf. –48.1 ppm for free dmpe).

The low symmetry isomers of **6** and **7** feature an Mn*H* ^{1}H NMR environment at –11.7 ppm with a very complex coupling pattern, and five ^{31}P NMR signals (40.9-76.1 ppm) attributed to the five inequivalent phosphine donors attached to manganese (in compound **7**, the pendant phosphine of the κ^1-dmpe ligand also gives rise to a sharp doublet at –49.1 ppm in the ^{31}P{^{1}H} NMR spectrum). These features are consistent with a disphenoidal arrangement of the chelating dmpe ligands, and *cis*-disposed hydride and μ-dmpe or κ^1-dmpe ligands; for monometallic **7**, *cis*-[(dmpe)$_2$MnH(κ^1-dmpe)] (***cis*-7**), and for

dimetallic **6**, either *cis*,*cis*-[{(dmpe)$_2$MnH}$_2$(μ-dmpe)] (***cis*,*cis*-6**) or *cis*,*trans*-[{(dmpe)$_2$MnH}$_2$(μ-dmpe)] (***cis*,*trans*-6**).[§§]

To demonstrate the generality of the aforementioned synthetic route to pentaphosphine manganese(I) hydride complexes, [(dmpe)$_2$MnH(C$_2$H$_4$)] (**1**) was exposed to an excess of PMe$_3$ under an atmosphere of H$_2$ for six days at 60 °C, yielding [(dmpe)$_2$MnH(PMe$_3$)] (**8**); Scheme 5. Analogous to the situation for **6**-**7**, compound **8** exists in solution as two isomers with *trans*- and *cis*- disposed PMe$_3$ and hydride ligands. Also, as with **6** and **7**, upon initial dissolution, the solution contained primarily the *trans* isomer (>95 %). In solution, photochemical *trans* to *cis* isomerization was observed; after 1 week at room temperature under ambient lab lighting, the *cis*:*trans* ratio was >3:1 (some deuterium incorporation into the alkyl and hydride environments was observed from C$_6$D$_6$ activation; [(dmpe)$_2$MnH(H$_2$)] (**2**) is known to activate C$_6$D$_6$ at elevated temperature or upon irradiation, likely via intermediate **B**).[40] Upon leaving this mixture of *cis*- and *trans*-**8** in the dark, the *trans* isomer was the dominant species in solution after 5 days at room temperature. Alternatively, heating the *cis*/*trans* mixture at 60 °C for 12 hours resulted in nearly complete conversion back to the *trans* isomer. The presence of ~10 equiv. of PMe$_3$ did not have a substantial effect on the rate of the photochemical or thermally-induced isomerization processes, though activation of C$_6$D$_6$ was supressed.

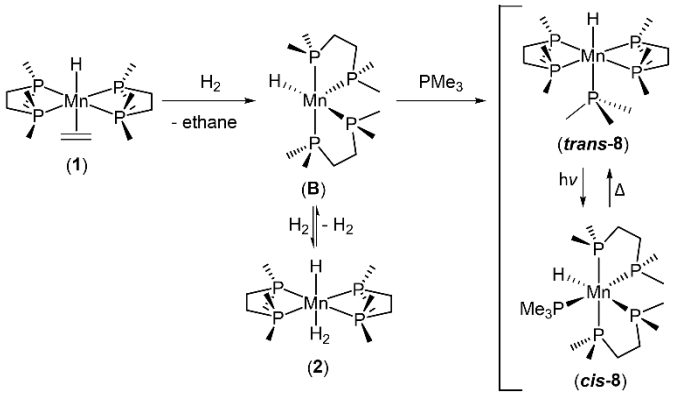

Scheme 5 Reaction of [(dmpe)$_2$MnH(C$_2$H$_4$)] (**1**) with PMe$_3$ under H$_2$ to generate phosphine hydride complex [(dmpe)$_2$MnH(PMe$_3$)] (**8**). Only one isomer is shown for **B**.

Recrystallization of reaction mixtures containing [{(dmpe)$_2$MnH}$_2$(μ-dmpe)] (**6**) from hexanes or hexamethyldisiloxane at –30 °C afforded X-ray quality crystals of ***trans*,*trans*-6** and ***cis*,*cis*-6**, respectively. Both of these structures (Figure 6) feature two octahedral Mn centres separated by a bridging dmpe ligand, with the remaining five coordination sites occupied by two chelating dmpe ligands and a hydride (one hydride ligand was not located from the difference map in ***cis*,*cis*-6**). The structure of ***trans*,*trans*-6** (Figure 6; top) features *trans*-disposed μ-dmpe and hydride ligands, and each octahedral Mn core is related by an inversion centre. The Mn–P distances are 2.2055(4)-2.2138(4) Å for the two chelating dmpe ligands, which are significantly shorter than the Mn–P distance of 2.2331(4) Å to the bridging dmpe ligand, likely reflecting the higher *trans* influence of hydride vs phosphine ligands. In contrast, the structure of ***cis*,*cis*-6** (Figure 6; bottom) features *cis* μ-dmpe and hydride ligands. However, the crystals were of poor quality, and the structure is only suitable to establish connectivity.

X-ray quality crystals of *trans*-[(dmpe)$_2$MnH(κ^1-dmpe)] (***trans*-7**) and *trans*-[(dmpe)$_2$MnH(PMe$_3$)] (***trans*-8**) (Figure 7) were obtained from concentrated solutions of **7** and **8** in O(SiMe$_3$)$_2$ or hexanes, respectively, at –30 °C. The environment at the metal centre is qualitatively analogous to that in the X-ray crystal structure of ***trans*,*trans*-6**, with *trans*-disposed hydride and κ^1-phosphine ligands. Despite the vast number of transition metal dmpe complexes, ***trans*-7** is, to our knowledge, only the second crystallographically characterized example with a κ^1-coordinated terminal dmpe ligand.[41]

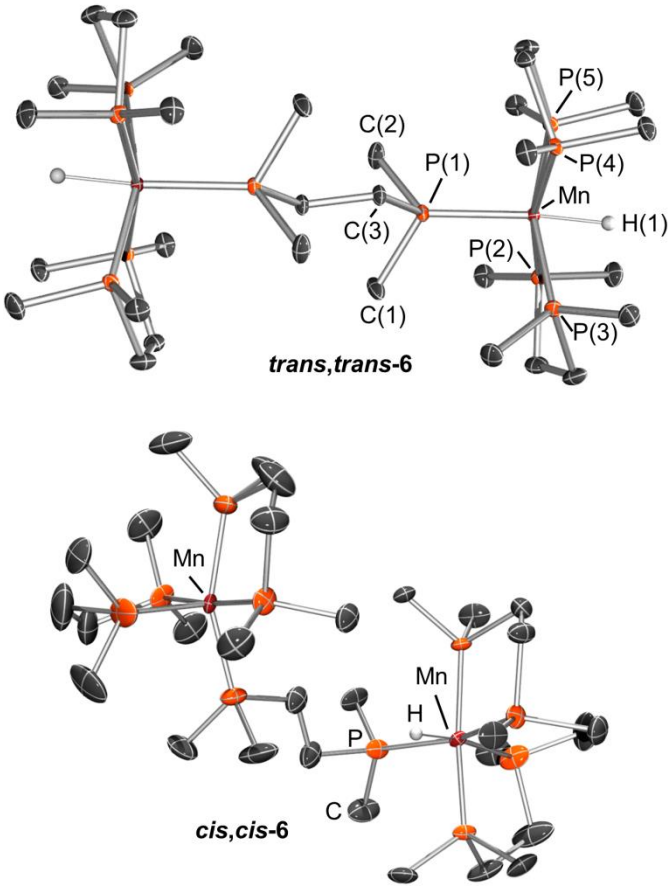

Figure 6 X-ray crystal structures of *trans*,*trans*-[{(dmpe)$_2$MnH}$_2$(μ-dmpe)] (***trans*,*trans*-6**, top) and *cis*,*cis*-[{(dmpe)$_2$MnH}$_2$(μ-dmpe)] (***cis*,*cis*-6**, bottom), with ellipsoids at 50 % probability. Most hydrogen atoms have been omitted for clarity. Hydrogen atoms on Mn were located from the difference map, with the exception of H on one of the Mn atoms of ***cis*,*cis*-6**, and refined isotropically. For ***trans*,*trans*-6**, distances (Å) and angles (deg): Mn(1)–P(1) 2.2331(4), Mn(1)–P(2) 2.2138(4), Mn(1)–P(3) 2.2065(4), Mn(1)–P(4) 2.2114(4), Mn(1)–P(5) 2.2055(4), Mn(1)–H(1) 1.53(1), P(1)–Mn(1)–H(1) 174.8(6), Σ(P–Mn–P) (*cis*, equatorial) 355.02(2). For ***cis*,*cis*-6**, all dmpe ligands are disordered over two positions, and only the major conformation (84.3(2) %) is shown. The crystal structure of ***cis*,*cis*-6** is of poor quality and is only suitable to determine connectivity.

Complexes **6**-**8** feature extremely electron-rich metal centres, and thus non-acidic hydride moieties; the pK_a^{LAC} (calculated using Morris' additive ligand acidity constant equation) for these complexes is 60.5, which is much higher than that for the vast majority of transition metal hydride complexes.[42] Complexes **6**-**8** are the first manganese hydride

complexes with five phosphine donors to be crystallographically characterized. Furthermore, the only spectroscopically characterized example, $[(F_3P)_5MnH]$,[43] differs significantly from **6**-**8** from an electronic standpoint, since PF_3 is a strong π-acceptor ligand comparable to carbon monoxide.

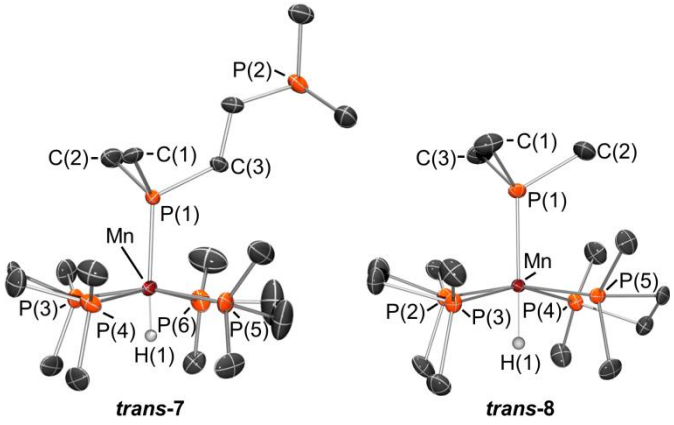

Figure 7 X-ray crystal structures of *trans*-$[(dmpe)_2MnH(\kappa^1\text{-dmpe})]$ (***trans*-7**, left) and *trans*-$[(dmpe)_2MnH(PMe_3)]$ (***trans*-8**, right), with ellipsoids drawn at 50 % probability. Most hydrogen atoms have been omitted for clarity. In the case of ***trans*-7**, the unit cell contains four independent and essentially isostructural molecules, only one of which is shown. Hydrogen atoms on Mn were located from the difference map, with the exception of H on Mn(1C) in ***trans*-7**, and refined isotropically. For ***trans*-7** (atoms with a letter suffix are related to those with the same identifying number without a suffix, but are located in one of the isostructural molecules in the unit cell), distances (Å) and angles (deg): Mn(1)–P(1) 2.231(4), Mn(1A)–P(1A) 2.230(4), Mn(1B)–P(1B) 2.232(4), Mn(1C)–P(1C) 2.234(4), Mn(1)–P(3) 2.211(4), Mn(1A)–P(3A) 2.201(5), Mn(1B)–P(3B) 2.190(4), Mn(1C)–P(3C) 2.228(4), Mn(1)–P(4) 2.212(4), Mn(1A)–P(4A) 2.222(5), Mn(1B)–P(4B) 2.220(4), Mn(1C)–P(4C) 2.216(4), Mn(1)–P(5) 2.214(4), Mn(1A)–P(5A) 2.213(5), Mn(1B)–P(5B) 2.224(4), Mn(1C)–P(5C) 2.211(4), Mn(1)–P(6) 2.213(4), Mn(1A)–P(6A) 2.203(4), Mn(1B)–P(6B) 2.211(4), Mn(1C)–P(6C) 2.203(4), Mn(1)–H(1) 1.16(6), Mn(1A)–H(1A) 1.16(7), Mn(1B)–H(1B) 1.16(6), P(1)–Mn(1)–H(1) 161(4), P(1A)–Mn(1A)–H(1A) 173(4), P(1B)–Mn(1B)–H(1B) 166(3), Σ(P–Mn(1)–P) (*cis*, equatorial) 355.1(4), Σ(P–Mn(1A)–P) (*cis*, equatorial) 355.0(4), Σ(P–Mn(1B)–P) (*cis*, equatorial) 355.6(4), Σ(P–Mn(1C)–P) (*cis*, equatorial) 355.0(4). For ***trans*-8**, distances (Å) and angles (deg): Mn(1)–P(1) 2.234(1), Mn(1)–P(2) 2.216(2), Mn(1)–P(3) 2.218(1), Mn(1)–P(4) 2.225(1), Mn(1)–P(5) 2.215(1), Mn(1)–H(1) 1.35(6), P(1)–Mn(1)–H(1) 179(2), Σ(P–Mn–P) (*cis*, equatorial) 355.3(1).

Summary and Conclusions

Borohydride complexes $[(dmpe)_2Mn(\mu\text{-}H)_2BR_2]$ ($R_2 = H_2$ (**3**), C_8H_{14} (**4**), and Mes_2 (**5**)) were accessed via the reactions of *trans*-$[(dmpe)MnH(C_2H_4)]$ (**1**) with either $BH_3(NMe_3)$ or HBR_2 ($R_2 = C_8H_{14}$ or Mes_2). The former reaction involves straightforward ethylene substitution. By contrast, the reaction with $HBMes_2$ (and likely also 9-BBN) proceeds via initial isomerization to form $[(dmpe)_2MnEt]$ (**A**), reaction of **A** with one equiv. of HBR_2 to afford $EtBR_2$ and $[(dmpe)_2MnH]$ (**B**), and reaction of **B** with a second equiv. of HBR_2 to afford the borohydride product. This reaction pathway (via intermediate **A**) mirrors that reported for reactions of **1** with hydrosilanes and dihydrogen.

$[(dmpe)_2Mn(\mu\text{-}H)_2BR_2]$ (R = H (**3**), $R_2 = C_8H_{14}$ (**4**), and R = Mes (**5**)) were identified as κ^2-borohydride complexes, as opposed to boryl dihydride or σ-hydroborane hydride isomers, by their low-frequency ^{11}B NMR chemical shifts (**3**: 25.3 ppm, **4**: 43.2 ppm, **5**: 27.5 ppm), long Mn–B distances (2.170(4)-2.245(3) Å), near-linear angles between Mn, B, and the centroid between the terminal substituents on boron, and DFT calculations (including Atoms in Molecules analysis). These Mn(I) borohydride complexes contrast the products formed in previously reported reactions of **1** with primary hydrosilanes, where partial Si–H bond oxidative addition is observed (to afford disilyl hydride complexes with appreciable bonding character between the hydride and silyl ligands). Complexes **4** and **5** are the first crystallographically characterized examples of manganese(I) borohydride complexes with two terminal hydrocarbyl substituents on boron.

Pentaphosphino hydride complexes $[\{(dmpe)_2MnH\}_2(\mu\text{-dmpe})]$ (**6**) and $[(dmpe)_2MnH(\kappa^1\text{-dmpe})]$ (**7**) were formed as decomposition products in the reactions to prepare **3**-**5**. These complexes, as well as $[(dmpe)_2MnH(PMe_3)]$ (**8**), were prepared independently from **1** by exposure to free dmpe or PMe_3 under an atmosphere of Ar or H_2; reactions under H_2 proceeded with initial ethane elimination to form $[(dmpe)_2MnH]$ (**B**), allowing for lower reaction temperatures and shorter reaction times. Compounds **6**-**8** can exist as isomers with *cis*- or *trans*-disposed hydride and κ^1-PR_3 ligands, and afford a remarkably high pK_a^{LAC} value of 60.5. The only other isolated (though not crystallographically characterized) pentaphosphine manganese hydride complex is $[(F_3P)_5MnH]$, which differs substantially from an electronic standpoint.

Experimental

General Methods. An argon-filled MBraun UNIlab glove box equipped with a –30 °C freezer was employed for the manipulation and storage of all oxygen- and moisture-sensitive compounds. Air-sensitive preparative reactions were performed on a double-manifold high-vacuum line equipped with a two stage Welch 1402 belt-drive vacuum pump (ultimate pressure 1×10^{-4} Torr) using standard techniques.[44] The vacuum was measured periodically using a Kurt J. Lesker 275i convection enhanced Pirani gauge. Residual oxygen and moisture was removed from the argon stream by passage through an Oxisorb-W scrubber from Matheson Gas Products.

Benzene, diethylether, hexamethyldisiloxane, and 1,2-diemethoxyethane (DME) were purchased from Aldrich, hexanes, toluene, and THF were purchased from Caledon, and deuterated solvents were purchased from ACP Chemicals. Benzene, diethylether, THF, DME, hexamethyldisiloxane, hexanes and toluene were initially dried and distilled at atmospheric pressure from sodium/benzophenone (first six) and sodium (toluene). All solvents were stored over an appropriate drying agent (hexamethyldisiloxane, benzene, diethylether, toluene, THF, DME, d_8-toluene, C_6D_6 = Na/Ph_2CO; hexanes = Na/Ph_2CO/tetraglyme) and introduced to reactions or solvent storage flasks via vacuum transfer with condensation at –78 °C.

PMe_3, dmpe, D_2, ethylene, 1,4-dioxane, 2-mesitylmagnesium bromide solution (1.0 M in THF), $BH_3(NMe_3)$, 9-BBN, $BF_3(Et_2O)$, $LiAlH_4$, $LiAlD_4$, and ethylmagnesium chloride solution (2.0 M in diethyl ether) were purchased from Sigma-Aldrich. Manganese dichloride

was purchased from Strem Chemicals. All reagents were used as purchased except 9-BBN which was purified by two successive recrystallizations from concentrated solutions in DME at –30 °C. Argon and hydrogen gas were purchased from PraxAir. [(dmpe)$_2$MnH(C$_2$H$_4$)] (**1**)[1,2] and HBMes$_2$[45] were prepared according to the literature. DBMes$_2$ was prepared in a manner analogous to HBMes$_2$, using LiAlD$_4$ in place of LiAlH$_4$.

NMR spectroscopy was performed on Bruker AV-500 and AV-600 spectrometers. Spectra were obtained at 298 K unless otherwise indicated. All ^{1}H NMR spectra were referenced relative to SiMe$_4$ through a resonance of the protio impurity of the solvent: C$_6$D$_6$ (δ 7.16 ppm) and *d*$_8$-toluene (δ 2.08 , 6.97, 7.01, and 7.09 ppm). All ^{2}H NMR spectra were referenced relative to the solvent: C$_6$D$_6$ (δ 7.16 ppm). All ^{13}C NMR spectra were referenced relative to SiMe$_4$ through a resonance of the solvent: C$_6$D$_6$ (δ 128.06 ppm) and *d*$_8$-toluene (δ 20.43, 125.13, 127.96, 128.87, and 137.48 ppm). The ^{11}B NMR spectra were referenced using an external standard of neat BF$_3$(Et$_2$O) (0.0 ppm), and the ^{31}P NMR spectra were referenced using an external standard of 85 % H$_3$PO$_4$ in D$_2$O (0.0 ppm) or by indirect referencing from a ^{1}H NMR spectrum.[46] NMR chemical shift abbreviations: s = singlet, d = doublet, t = triplet, q = quartet, quin. = quintet, m = multiplet, app. = apparent, br. = broad. Combustion elemental analyses were performed by the London Metropolitan University in London, UK, and Midwest Microlabs in Indianapolis.

Single-crystal X-ray crystallographic analyses were performed on crystals coated in Paratone oil and mounted on a Bruker SMART APEX II diffractometer with a 3 kW sealed-tube Mo generator and APEX II CCD detector in the McMaster Analytical X-Ray (MAX) Diffraction Facility. A semi-empirical absorption correction was applied using redundant and symmetry related data. Raw data was processed using XPREP (as part of the APEX v2.2.0 software), and solved by either direct (SHELXS-97)[47] or intrinsic (SHELXT)[48] methods. Structures were completed by difference Fourier synthesis and refined with full-matrix least-squares procedures based on F^2. In all cases, non-hydrogen atoms were refined anisotropically and hydrogen atoms were generated in ideal positions and then updated with each cycle of refinement (with the exception of hydrogen atoms on Mn or B, which were located from the difference map and refined isotropically). Refinement was performed with SHELXL[49] in Olex2.[50] For ***trans*-7**, the initial cell gave a whole-molecule disordered solution. MAX3D[51] was used to visualize the three dimensional diffraction pattern, indicating the presence of very weak interleaving layers of diffraction. This allowed a new supercell to be determined (1 0 1, 0 -1 0, -1 0 1) which could be refined with no disorder.

Details on computational methods can be found in the electronic supporting information.

All prepared complexes are air sensitive, and their products upon reaction with air are malodorous. Therefore, all syntheses were conducted under an atmosphere of argon.

[(dmpe)$_2$Mn(μ-H)$_2$BH$_2$] (3). 225 mg (0.58 mmol) of [(dmpe)$_2$MnH(C$_2$H$_4$)] (**1**) and an excess of BH$_3$(NMe$_3$) (64 mg, 0.88 mmol) were dissolved in 50 mL of toluene, and the resulting yellow solution was placed in a sealed 100 mL storage flask and stirred at 90 °C. After 2 days of heating, the dark purple solution was briefly cooled to room temperature, and exposed to dynamic vacuum for a few seconds to remove some ethylene byproduct. After an additional 2 days of stirring at 90 °C, the solvent was removed *in vacuo*. The resulting dark purple solid was placed under vacuum for an hour at room temperature to remove excess BH$_3$(NMe$_3$), and the crude product was recrystallized from hexanes at –30 °C to afford deep purple crystals which were dried *in vacuo* (64 mg, 30 %). X-ray quality crystals were obtained from a concentrated solution in hexanes at –30 °C. **T$_{sublimation}$ (5 mTorr):** 80-85 °C. **^{1}H NMR (*d*$_8$-toluene, 600 MHz, 298 K):** δ 5.08 (m, 2H, Mn(μ-H)$_2$B*H*$_2$), 1.69, 1.16 (2 × m, 2H, PC*H*$_2$), 1.60, 1.43 (2 × m, 6H, PC*H*$_3$), 1.34 (m, 4H, PC*H*$_2$), 0.97 (d, 6H, $^2J_{H,P}$ 5.8 Hz, PC*H*$_3$), 0.71 (d, 6H, $^2J_{H,P}$ 5.2 Hz, PC*H*$_3$), –16.52 (m, 2H, Mn(μ-*H*)$_2$BH$_2$). **^{11}B{^{1}H} NMR (*d*$_8$-toluene, 192 MHz, 298 K):** δ 25.30 (s). **^{13}C{^{1}H} NMR (*d*$_8$-toluene, 151 MHz, 298 K):** δ 33.48, 32.78 (2 × m, PCH$_2$), 29.12, 23.25 (2 × m, PCH$_3$), 21.82 (s, PCH$_3$), 20.21 (PCH$_3$)¶¶. **^{31}P{^{1}H} NMR (*d*$_8$-toluene, 243 MHz, 298 K):** δ 88.56, 72.54 (2 × s). **Anal.** Found (calcd): C, 38.99 (38.95); H, 9.64 (9.81).

[(dmpe)$_2$Mn(μ-H)$_2$BC$_8$H$_{14}$] (4). Method a) 10.3 mg (0.03 mmol) of [(dmpe)$_2$MnH(C$_2$H$_4$)] (**1**) and two equivalents of 9-BBN (6.5 mg, 0.05 mmol) were dissolved in approx. 0.6 mL of C$_6$D$_6$, and the resulting yellow solution was heated at 60 °C for 12 hours. The resulting deep red solution was analyzed *in situ* by NMR spectroscopy to have resulted in >95 % consumption of **1** to form [(dmpe)$_2$Mn(μ-H)$_2$BC$_8$H$_{14}$] (**4**), along with numerous byproducts. Method b) 73.7 mg (0.60 mmol) of 9-BBN was added to a solution of 116 mg (0.30 mmol) of [(dmpe)$_2$MnH(C$_2$H$_4$)] (**1**) in 20 mL of benzene, and the resulting solution was stirred at 90 °C overnight (with the solution turning from bright yellow to dark brown). The solvent was then removed *in vacuo*, and resulting black solid was dissolved in a minimal amount hexanes. Allowing this solution to stand at –30 °C yielded a mixture of yellow and red crystals; the former were *trans,trans*-[{(dmpe)$_2$MnH}$_2$(μ-dmpe)] (***trans,trans*-6**) while the latter was [(dmpe)$_2$Mn(μ-H)$_2$BC$_8$H$_{14}$] (**4**). Both sets of crystals were of X-ray quality. Picking out red crystals with tweezers allowed isolation of **4** in >99 % purity by NMR spectroscopy. Attempts to separate **4** and **6** on a preparative scale by preferential crystallization or sublimation were unsuccessful. For atom labels used in the following NMR assignments, consult Figure S14 in the ESI. **^{1}H NMR (C$_6$D$_6$, 600 MHz, 298 K):** δ 2.29 (app. nonet, 2H, $^3J_{H,H}$ 6.0 Hz, C*H*$_2$(C)), 2.13 (m, 8H, C*H*$_2$(B)), 1.86 (m, 2H, C*H*$_2$(C)), 1.67, 1.27 (2 × m, 2H, PC*H*$_2$), 1.55 (m, 6H, PC*H*$_3$), 1.40 (s, 6H, PC*H*$_3$), 1.36 (br. s, 2H, C*H*(A)), 1.23 (d, 6H, $^2J_{H,P}$ 5.2 Hz, PC*H*$_3$), 1.17 (m, 4H, PC*H*$_2$), 0.72 (d, 6H, $^2J_{H,P}$ 4.7 Hz, PC*H*$_3$), –15.55 (br. s, 2H, Mn(μ-*H*)$_2$BR$_2$). **^{11}B{^{1}H} NMR (C$_6$D$_6$, 192 MHz, 298 K):** δ 43.16 (s). **^{13}C{^{1}H} NMR (C$_6$D$_6$, 151 MHz, 298 K):** δ 36.96 (m, *C*H(A)), 35.94 (m, PCH$_2$), 35.39, 34.32 (2 × s, *C*H$_2$(B)), 31.25 (m, PCH$_2$ and PCH$_3$), 25.00 (s, *C*H$_2$(C)), 24.91 (m, PCH$_3$), 23.80, 20.79 (2 × s, PCH$_3$). **^{31}P{^{1}H} NMR (C$_6$D$_6$, 243 MHz, 298 K):** δ 85.08, 70.11 (2 × s).

[(dmpe)$_2$Mn(μ-H)$_2$BMes$_2$] (5). 172.0 (0.69 mmol) of HBMes$_2$ and 132.1 mg (0.34 mmol) of [(dmpe)$_2$MnH(C$_2$H$_4$)] (**1**) were dissolved in 20 mL of toluene, and the resulting solution

was stirred at 60 °C for two days (turning from bright yellow to dark purple). The solvent was then removed *in vacuo*, and the resulting purple solid was washed with 10 mL of hexanes, 3 mL of toluene, and dissolved in 12 mL of toluene. The toluene solution was layered with 3 mL of hexanes and stored for days at –30 °C, after which 48.8 mg of a very dark purple solid (both crystals and powder) had crystallized. To obtain a higher yield, the solvent was removed *in vacuo* from the mother liquor, and the resulting solid dissolved in 2 mL of THF which was allowed to sit for days at –30 °C, affording an additional 22.0 mg of **5** as purple crystals (combined yield of 70.8 mg, 0.12 mmol, 34 %). X-ray quality crystals were obtained by performing the reaction in a J Young NMR tube at 60 °C in C_6D_6 (using 10.0 mg of **1** and 13.0 mg of $HBMes_2$). **^{1}H NMR (d_8-toluene, 600 MHz, 298 K):** δ 6.92, 6.61 (2 × s, 2H, *m*-C*H*), 2.84, 2.26 (2 × s, 6H, *o*-CH_3), 2.23 (s, 6H, *p*-CH_3), 1.51 (m, 2H, PCH_2), 1.38, 0.70 (2 × m, 6H, PCH_3), 1.26 (d, 6H, $^2J_{H,P}$ 5.4 Hz, PCH_3), 1.08 (m, 6H, PCH_2), 0.65 (d, 6H, $^2J_{H,P}$ 4.8 Hz, PCH_3), –13.98 (br. s, 2H, Mn(μ-H)$_2$BR_2). **^{11}B{^{1}H} NMR (d_8-toluene, 192 MHz, 298 K):** δ 27.46 (s). **^{13}C{^{1}H} NMR (d_8-toluene, 151 MHz, 298 K):** 153.3 (*ipso*-*C*),¶¶ 140.73, 140.21 (2 × s, *o*-*C*Me) 133.60 (s, *p*-*C*Me) 129.1, 128.7 (2 × *m*-C*H*),¶¶ 37.11, 32.00 (2 × m, P*C*H$_2$), 27.51, 25.24 (2 × s, *o*-*C*H$_3$), 27.51 (s, P*C*H$_3$), 24.75, 21.25 (2 × m, P*C*H$_3$), 21.13 (s, *p*-*C*H$_3$), 20.0 (P*C*H$_3$).¶¶ **^{31}P{^{1}H} NMR (d_8-toluene, 243 MHz, 298 K):** δ 85.82, 62.61 (2 × s). **Anal.** Found (calcd.): C, 59.38 (59.42); H, 9.37 (9.31).

[(dmpe)$_2$Mn(μ-D)$_2$BMes$_2$] (d_2-5). 11.7 mg (0.03 mmol) of [(dmpe)$_2$MnH(C_2H_4)] (**1**) and 15.3 mg (0.06 mmol) of $DBMes_2$ were dissolved in approx. 0.6 mL of C_6D_6. The resulting solution was heated overnight at 60 °C, and analyzed by NMR spectroscopy *in situ*. ^{1}H and ^{11}B{^{1}H} NMR data match that of **5**, with the exception of no ^{1}H NMR signal in the Mn(μ-*H*)$_2$BH_2 region. **^{2}H NMR (C_6D_6, 77 MHz, 298 K):** δ –14.09 (s, Mn*D*).

Reaction of [(dmpe)$_2$Mn(μ-H)$_2$BH_2] (3) with D_2. Approximately 10 mg of [(dmpe)$_2$Mn(μ-H)$_2$BH_2] (**3**) was dissolved in roughly. 0.6 mL of C_6D_6. The reaction mixture was freeze/pump/thaw cycled in a J. Young NMR tube three times and then placed under 1 atm of D_2 at –95 °C, sealed, and warmed to room temperature. After heating at 90 °C for 12 h, the resulting solution was analyzed by NMR spectroscopy *in situ*. ^{1}H NMR data matches that for **3**, with 40 % reduction in the relative intensity of both the Mn(μ-*H*)$_2$BH_2 and Mn(μ-H)$_2$B*H*$_2$ environments, accompanied by H_2 and HD in an approximate 1:8 ratio. The integral for the C_6D_5H environment (relative to that for the combined alkyl environments of **3**) in the ^{1}H NMR spectra of this reaction mixture did not increase during this reaction, indicating that C_6D_6 activation is not the source of the observed deuterium incorporation.

[{(dmpe)$_2$MnH}$_2$(μ-dmpe)] (6). 100 mg (0.26 mmol) of [(dmpe)$_2$MnH(C_2H_4)] (**1**) and a limiting amount of dmpe (18.1 mg, 0.12 mmol) were dissolved in 25 mL of toluene. The resulting yellow solution was freeze/pump/thaw cycled three times in a 100 mL storage flask, and was then placed under an atmosphere of hydrogen gas at –130 °C, sealed, and warmed to room temperature. After stirring the mixture for 4 days at 60 °C, the solvent was removed *in vacuo* yielding a yellow solid, which was twice washed with 4 mL of hexanes at –30 °C, then dried *in vacuo* at room temperature. Yield = 29.3 mg (0.03 mmol, 28 %). X-ray quality crystals of ***cis*,*cis*-6** were obtained from a concentrated solution of **6** in hexamethyldisiloxane at –30 °C, and X-ray quality crystals of ***trans*,*trans*-6** were obtained from a concentrated solution of **4** and **6** (formed from the crude reaction mixture in the synthesis of **4**; *vide supra*) in hexanes at –30 °C. NMR data for ***trans*,*trans*-6** are as follows: **^{1}H NMR (C_6D_6, 600 MHz, 298 K):** δ 1.66, 1.50 (2 × m, 8H, PCH_2-chelating), 1.48, 1.36 (2 × s, 24H, PCH_3-chelating), 1.30 (br. s, 4H, PCH_2-κ^1), 1.02 (d, $^2J_{H,P}$ 3.5 Hz, 12H, PCH_3-κ^1), –15.74 (quin. of d, 2H, $^2J_{H,P}$ 48.8 Hz, $^2J_{H,P}$ 12.5 Hz, Mn*H*). **^{13}C{^{1}H} NMR (C_6D_6, 126 MHz, 298 K)**: δ 36.70 (m, P*C*H$_2$-κ^1), 34.34 (app. quin., $J_{C,P}$ 11.8 Hz, P*C*H$_2$-chelating), 32.07 (br. s, P*C*H$_3$-chelating), 24.68 (s, P*C*H$_3$-chelating), 24.61 (s, P*C*H$_3$-κ^1). **^{31}P{^{1}H} NMR (C_6D_6, 243 MHz, 298 K):** δ 78.82 (s, 8P, chelating P), 26.37 (s, 2P, κ^1-P). Selected NMR data for ***cis*-containing 6** are as follows: **^{1}H NMR (C_6D_6, 600 MHz, 298 K):** δ –11.66 (m, Mn*H*). **^{31}P{^{1}H} NMR (C_6D_6, 243 MHz, 298 K):** δ 76.12, 75.23, 73.69, 63.85, 40.91 (5 × s). **Anal.** Found (calcd): C, 41.69 (41.77); H, 9.52 (9.58).

[(dmpe)$_2$MnH(κ^1-dmpe)] (7). 170 mg (0.44 mmol) of [(dmpe)$_2$MnH(C_2H_4)] (**1**) and an excess of dmpe (100 mg, 0.67 mmol) were dissolved in 50 mL of benzene. The resulting yellow solution was freeze/pump/thaw cycled three times in a 250 mL storage flask and was then placed under an atmosphere of hydrogen gas at –130 °C, sealed, and warmed to room temperature. After stirring the reaction mixture for 6 days at 60 °C, the solvent was removed *in vacuo*. The resulting yellow oil was heated at 50 °C *in vacuo* for 24 hours to remove volatile impurities, then sublimed at 100 °C to afford 77.4 mg of **7** as a yellow solid (0.15 mmol, 35 %). X-ray quality crystals of ***trans*-7** were obtained from a concentrated solution in hexamethyldisiloxane at –30 °C. NMR data for ***trans*-7** are as follows: **^{1}H NMR (C_6D_6, 600 MHz, 298 K):** δ 1.62, 1.47 (2 × m, 4H, PCH_2-chelating), 1.45, 1.34 (2 × s, 12H, PCH_3-chelating), 1.38, (m, 2H, MnP(Me)$_2$CH$_2$CH_2PMe$_2$), 1.28 (m, 2H, MnP(Me)$_2$CH_2CH$_2$PMe$_2$), 0.96 (d, 6H, $^2J_{H,P}$ 3.8 Hz, MnP(PCH_3)$_2$CH$_2$CH$_2$PMe$_2$), 0.89 (d, 6H, $^2J_{H,P}$ 2.8 Hz, MnP(Me)$_2$CH$_2$CH$_2$P(PCH_3)$_2$), –15.72 (quin. of d, 1H, $^2J_{H,P}$ 48.8 Hz, $^2J_{H,P}$ 12.9 Hz, Mn*H*). **^{13}C{^{1}H} NMR (C_6D_6, 151 MHz, 298 K):** δ 38.09 (s, MnP(Me)$_2$CH$_2$*C*H$_2$PMe$_2$), 34.33 (app. quin., $^1J_{C,P}$ 11.9 Hz, P*C*H$_2$-chelating), 32.02, 24.62 (2 × s, P*C*H$_3$-chelating), 26.50 (d of d, $^1J_{C,P}$ 13.4 Hz, $^2J_{C,P}$ 7.3 Hz, MnP(Me)$_2$*C*H$_2$CH$_2$PMe$_2$), 24.84 (d, $^1J_{C,P}$ 9.4 Hz, MnP(P*C*H$_3$)$_2$CH$_2$-CH$_2$PMe$_2$), 13.95 (d, $^1J_{C,P}$ 16.0 Hz, MnP(Me)$_2$CH$_2$CH$_2$P(P*C*H$_3$)$_2$). **^{31}P{^{1}H} NMR (C_6D_6, 243 MHz, 298 K):** δ 78.63 (s, 4P, chelating P), 27.64 (s, 1P, Mn*P*(Me)$_2$CH$_2$CH$_2$PMe$_2$), –49.61 (d, 1P, $^3J_{P,P}$ 14.1 Hz, MnP(Me)$_2$CH$_2$CH$_2$*P*Me$_2$). Selected NMR data for ***cis*-7** are as follows: **^{1}H NMR (C_6D_6, 600 MHz, 298 K):** δ –11.68 (m, Mn*H*). **^{31}P{^{1}H} NMR (C_6D_6, 243 MHz, 298 K):** δ 75.96, 75.06, 73.42, 63.65, 43.19 (5 × s), –49.13 (d, $^3J_{P,P}$ 18.7 Hz, MnP(Me)$_2$CH$_2$CH$_2$*P*Me$_2$). **Anal.** Found (calcd): C, 42.84 (42.70); H, 9.82 (9.75).

[(dmpe)$_2$MnH(PMe$_3$)] (8). An excess of PMe_3 (1.54 g, 20.2 mmol) was distilled into a 250 mL storage flask containing

2.03 g (5.28 mmol) of [(dmpe)$_2$MnH(C$_2$H$_4$)] (**1**) in 100 mL of benzene. The resulting yellow solution was freeze/pump/thaw cycled three times and was then placed under an atmosphere of hydrogen gas at –95 °C, sealed, and warmed to room temperature. After stirring the mixture for 4 days at 60 °C, the solution was frozen and headspace evacuated. Additional PMe$_3$ (0.62 g, 8.15 mmol) was distilled into the reaction flask (containing the still-frozen solution), which was then placed under an atmosphere of hydrogen gas at –95 °C, sealed, and warmed to room temperature. The reaction mixture was stirred for an additional 48 hours at 60 °C, after which the solvent was removed *in vacuo* to afford 2.10 g of **8** as a yellow solid (4.86 mmol, 92 %). X-ray quality crystals of ***trans*-8** were obtained from a concentrated solution in hexanes at –30 °C. **$T_{sublimation}$ (5 mTorr)** = 60 °C. NMR data for ***trans*-8** are as follows: **^{1}H NMR (C$_6$D$_6$, 600 MHz, 298 K):** δ 1.61, 1.42 (2 × m, 4H, PC$\underline{H}_2$), 1.42, 1.34 (2 × s, 12H, dmpe-PC$\underline{H}_3$), 1.02 (d, $^2J_{H,P}$ 4.2 Hz, 9H, PMe$_3$-PC$\underline{H}_3$), –15.52 (quin. of d, $^2J_{H,P}$ 48.7 Hz, $^2J_{H,P}$ 13.7 Hz, 1H, Mn$\underline{H}$). **^{13}C{^{1}H} NMR (C$_6$D$_6$, 126 MHz, 298 K)**: δ 34.19 (app. quin., $J_{C,P}$ 12.2 Hz, dmpe-P$\underline{C}$H$_2$), 31.84, 24.35 (2 × m, dmpe-P$\underline{C}$H$_3$), 30.90 (d, $^1J_{C,P}$ 12.0 Hz, PMe$_3$-P$\underline{C}$H$_3$). **^{31}P{^{1}H} NMR (C$_6$D$_6$, 243 MHz, 298 K):** δ 79.13 (s, 4P, dmpe-$\underline{P}$), 19.01 (s, 1P, $\underline{P}$Me$_3$). NMR data for ***cis*-8** are as follows: **^{1}H NMR (C$_6$D$_6$, 600 MHz, 298 K):** δ 1.74, 1.62 (2 × m, 2H, PC$\underline{H}_2$), 1.53 (d, $^2J_{H,P}$ 5.4 Hz, 3H, dmpe-PC$\underline{H}_3$), 1.43, 1.42 (2 × m, 3H, dmpe-PC$\underline{H}_3$), 1.37, 1.22 (2 × d, $^2J_{H,P}$ 4.7 Hz, 3H, dmpe-PC$\underline{H}_3$), 1.34, 1.22, 1.20, 0.90 (4 × m, 1H, PC$\underline{H}_2$), 1.29 (d, $^2J_{H,P}$ 5.0 Hz, 9H, PMe$_3$-PC$\underline{H}_3$), 1.20 (d, $^2J_{H,P}$ 4.3 Hz, 3H, dmpe-PC$\underline{H}_3$), 1.18 (d, $^2J_{H,P}$ 4.4 Hz, 3H, dmpe-PC$\underline{H}_3$), 1.04 (d, $^2J_{H,P}$ 4.1 Hz, 3H, dmpe-PC$\underline{H}_3$), –11.73 (m, 1H, Mn$\underline{H}$). **^{13}C{^{1}H} NMR (C$_6$D$_6$, 126 MHz, 298 K)**: δ 36.70, 35.13, 34.54 (3 × m, P$\underline{C}$H$_2$), 31.97 (m, dmpe-P$\underline{C}$H$_3$),¶¶ 30.32 (d, $^1J_{C,P}$ 13.9 Hz, PMe$_3$-P$\underline{C}$H$_3$), 28.10, 27.79, 26.09, 24.84, 24.51 (5 × m, dmpe-P$\underline{C}$H$_3$), 25.02 (s, dmpe-P$\underline{C}$H$_3$). **^{31}P{^{1}H} NMR (C$_6$D$_6$, 243 MHz, 298 K):** δ 76.23 (s, 2P, dmpe-$\underline{P}$), 74.85, 63.90 (2 × s, 1P, dmpe-$\underline{P}$), 31.23 (s, 1P, $\underline{P}$Me$_3$). **Anal.** found (calcd): C, 41.54 (41.67); H, 9.67 (9.79).

Monitoring *trans–cis* isomerization of [(dmpe)$_2$MnH(PMe$_3$)] (8). 55 mg of ***trans*-8** was dissolved in approximately 3 mL of C$_6$D$_6$, and four 0.6 mL aliquots of this solution were placed in individual J-young NMR tubes. Two of the four solutions were frozen at –78 °C, and ~ 10 equivalents of PMe$_3$ were introduced by vacuum transfer. Two solutions were kept in the dark (one with and one without excess PMe$_3$), while the other two (one with and one without excess PMe$_3$) were placed in a fume hood with the light on. All four solutions were monitored over time by ^{1}H, ^{2}H, and ^{31}P{^{1}H} NMR spectroscopy. Only the solutions stored in the light underwent *trans* to *cis* isomerization, and after 2 weeks at room temperature, these solutions were placed in the dark to monitor the reverse reaction (*cis* to *trans* isomerization).

Conflicts of interest

There are no conflicts to declare.

Acknowledgements

D. J. H. E. thanks NSERC of Canada for a Discovery Grant.

Notes and References

‡ In the reactions of **1** with either 9-BBN or HBMes$_2$, two intermediates were observed concurrently by NMR spectroscopy. NMR spectra of one intermediate displayed high symmetry consistent with an equatorial arrangement of chelating dmpe donors, and spectra of the other displayed low symmetry consistent with a disphenoidal arrangement of chelating dmpe donors. In the reaction to form [(dmpe)$_2$Mn(μ-H)$_2$BC$_8$H$_{14}$] (**4**), the low symmetry species is dominant, whereas in the reaction to form [(dmpe)$_2$Mn(μ-H)$_2$BMes$_2$] (**5**), the high symmetry species is dominant.

§ Ethylene was found to insert into the B–H bond of free 9-BBN or HBMes$_2$, with 90 % (9-BBN reaction) or 100 % (HBMes$_2$ reaction) conversion to EtBR$_2$ after 1 h at 60 °C in C$_6$D$_6$ under an initial atmosphere of 1.7 atm ethylene. An alternative mechanism for ethylene hydroboration could be envisaged involving complex **5** as a catalyst (involving H$_2$ elimination from **5** followed by ethylene coordination and B–C bond forming 1,2-insertion), though such reactivity would also result in a deuterium distribution inconsistent with experimental observations.

¶ Octahedral, 18-electron, low-spin d^6 complexes of 1st row transition metals are unlikely to undergo associative substitution. Therefore, the reaction of **1** with BH$_3$(NMe$_3$) likely proceeds by initial ethylene dissociation (from either the *trans* or the *cis* isomer of **1**) to form a 5-coordinate hydride intermediate [(dmpe)$_2$MnH] (**B**), followed by BH$_3$(NMe$_3$) coordination. It is likely that ethylene dissociation occurs from the *trans* isomer of **1**, given that this isomer is dominant in solution, and considering the high *trans* influence of hydride ligands (see reference 3).

| The quadrupolar relaxation rate is proportional to the rotational correlation time (τ_c). The rotational correlation time can be described using the Stokes' equation $\tau_c = 4\pi a^3\eta^*/3kT$, where a = molecular radius, η* = viscosity, k = Boltzmann's constant, and T = temperature. See reference 36.

†† The borohydride ligand in one of Figueroa's borohydride crystal structures (ref. 25) is disordered over two positions. This Mn–B range does not include the Mn–B distance of 2.08(3) Å involving the minor (18 %) disorder, because the large standard deviation precludes meaningful discussion.

‡‡ The angle between Mn, B, and the centroid between the two terminal H atoms on B in complex **3** is 173.6°, though it is based on the location of hydrogen atoms in the X-ray crystal structure, and could thus be inaccurate. The angle in the geometry optimized (DFT) structure of **3** is 179.7°.

§§ If the observed signals are due to ***cis*,*trans*-6**, all ^{31}P and Mn*H* ^{1}H NMR signals for the Mn centre with *trans* hydride and μ-dmpe ligands must overlap with those arising from ***trans*,*trans*-6**.

¶¶ Chemical shift located from a crosspeak in 2D NMR.

1 G. S. Girolami, G. Wilkinson, M. Thornton-Pett and M. B. Hursthouse, *J. Am. Chem. Soc.*, 1983, **105**, 6752-6753.
2 G. S. Girolami, C. G. Howard, G. Wilkinson, H. M. Dawes, M. Thornton-Pett, M. Motevalli and M. B. Hursthouse, *J. Chem. Soc., Dalton Trans.*, 1985, 921-929.
3 J. S. Price, D. J. H. Emslie, I. Vargas-Baca and J. F. Britten, *Organometallics*, 2018, **37**, 3010-3023.
4 J. S. Price, D. J. H. Emslie and J. F. Britten, *Angew. Chem., Int. Ed.*, 2017, **56**, 6223-6227.
5 (a) T. J. Marks and J. R. Kolb, *Chem. Rev.*, 1977, **77**, 263-293; (b) G. Alcaraz, M. Grellier and S. Sabo-Etienne, *Acc. Chem. Res.*, 2009, **42**, 1640-1649.
6 M. Besora and A. Lledós, in *Contemporary Metal Boron Chemistry I*, eds. T. B. Marder and Z. Lin, Springer, Berlin, 2008, pp. 149-202.
7 X.-Y. Liu, S. Bouherour, H. Jacobsen, H. W. Schmalle and H. Berke, *Inorg. Chim. Acta*, 2002, **330**, 250-267.
8 A. Rossin, M. Peruzzini and F. Zanobini, *Dalton Trans.*, 2011, **40**, 4447-4452.
9 J. F. Hartwig and S. R. De Gala, *J. Am. Chem. Soc.*, 1994, **116**, 3661-3662.
10 D. R. Lantero, D. L. Ward and M. R. Smith III, *J. Am. Chem. Soc.*, 1997, **119**, 9699-9708.
11 (a) T. Hascall, B. M. Bridgewater and G. Parkin, *Polyhedron*, 2000, **19**, 1063-1066; (b) A. Antiñolo, F. Carrillo-Hermosilla, J. Fernández-Baeza, S. García-Yuste, A. Otero, A. M. Rodríguez, J. Sánchez-Prada, E. Villaseñor, R. Gelabert, M. Moreno, J. M. Lluch and A. Lledós, *Organometallics*, 2000, **19**, 3654-3663; (c) K. Essalah, J.-C. Barthelat, V. Montiel, S. Lachaize, B. Donnadieu, B. Chaudret and S. Sabo-Etienne, *J. Organomet. Chem.*, 2003, **680**, 182-187; (d) M. C. Denney, V. Pons, T. J. Hebden, D. M. Heinekey and K. I. Goldberg, *J. Am. Chem. Soc.*, 2006, **128**, 12048-12049; (e) W. J. Evans, S. E. Lorenz and J. W. Ziller, *Chem. Commun.*, 2007, 4662-4664; (f) Y. Ohki, T. Hatanaka and K. Tatsumi, *J. Am. Chem. Soc.*, 2008, **130**, 17174-17186; (g) S. Bontemps, L. Vendier and S. Sabo-Etienne, *Angew. Chem., Int. Ed.*, 2012, **51**, 1671-1674; (h) S. Chakraborty, J. Zhang, Y. J. Patel, J. A. Krause and H. Guan, *Inorg. Chem.*, 2013, **52**, 37-47.
12 S. Lachaize, K. Essalah, V. Montiel-Palma, L. Vendier, B. Chaudret, J.-C. Barthelat and S. Sabo-Etienne, *Organometallics*, 2005, **24**, 2935-2943.
13 N. Arnold, S. Mozo, U. Paul, U. Radius and H. Braunschweig, *Organometallics*, 2015, **34**, 5709-5715.
14 C. Lenczyk, D. K. Roy, J. Nitsch, K. Radacki, F. Rauch, R. D. Dewhurst, F. M. Bickelhaupt, T. B. Marder and H. Braunschweig, *Chem. - Eur. J.*, 2019, **25**, 13566-13571.
15 (a) D. R. Lantero, D. H. Motry, D. L. Ward and M. R. Smith III, *J. Am. Chem. Soc.*, 1994, **116**, 10811-10812; (b) K. Kawamura and J. F. Hartwig, *J. Am. Chem. Soc.*, 2001, **123**, 8422-8423.
16 D. R. Lantero, S. L. Miller, J.-Y. Cho, D. L. Ward and M. R. Smith III, *Organometallics*, 1999, **18**, 235-247.
17 T. J. Hebden, M. C. Denney, V. Pons, P. M. B. Piccoli, T. F. Koetzle, A. J. Schultz, W. Kaminsky, K. I. Goldberg and D. M. Heinekey, *J. Am. Chem. Soc.*, 2008, **130**, 10812-10820.
18 D. Liu, K.-C. Lam and Z. Lin, *J. Organomet. Chem.*, 2003, **680**, 148-154.
19 (a) K. K. Pandey, *Inorg. Chem.*, 2001, **40**, 5092-5096; (b) T. Miyada, E. H. Kwan and M. Yamashita, *Organometallics*, 2014, **33**, 6760-6770.
20 J. C. Babón, M. A. Esteruelas, I. Fernández, A. M. López and E. Oñate, *Inorg. Chem.*, 2018, **57**, 4482-4491.
21 (a) K. Burgess, W. A. Van der Donk, S. A. Westcott, T. B. Marder, R. T. Baker and J. C. Calabrese, *J. Am. Chem. Soc.*, 1992, **114**, 9350-9359; (b) D. Adhikari, J. C. Huffman and D. J. Mindiola, *Chem. Commun.*, 2007, 4489-4491; (c) Y. Zhu, C.-H. Chen, C. M. Fafard, B. M. Foxman and O. V. Ozerov, *Inorg. Chem.*, 2011, **50**, 7980-7987.
22 G. Alcaraz, U. Helmstedt, E. Clot, L. Vendier and S. Sabo-Etienne, *J. Am. Chem. Soc.*, 2008, **130**, 12878-12879.
23 G. M. Adams, A. L. Colebatch, J. T. Skornia, A. I. McKay, H. C. Johnson, G. C. Lloyd−Jones, S. A. Macgregor, N. A. Beattie and A. S. Weller, *J. Am. Chem. Soc.*, 2018, **140**, 1481-1495.
24 (a) R. Carreño, V. Riera, M. A. Ruiz, Y. Jeannin and M. Philoche-Levisalles, *J. Chem. Soc., Chem. Commun.*, 1990, 15-17; (b) R. Carreño, V. Riera, M. A. Ruiz, C. Bois and Y. Jeannin, *Organometallics*, 1993, **12**, 1946-1953.
25 D. W. Agnew, C. E. Moore, A. L. Rheingold and J. S. Figueroa, *Organometallics*, 2017, **36**, 363-371 and personal communication from Dr. J. Figueroa.
26 D. H. Nguyen, X. Trivelli, F. Capet, J.-F. Paul, F. Dumeignil and R. M. Gauvin, *ACS Catal.*, 2017, **7**, 2022-2032.
27 R. Prakash, A. N. Pradhan, M. Jash, S. Kahlal, M. Cordier, T. Roisnel, J.-F. Halet and S. Ghosh, *Inorg. Chem.*, 2020, **59**, 1917-1927.
28 G. Jia, A. J. Lough and R. H. Morris, *J. Organomet. Chem.*, 1993, **461**, 147-156.
29 R. T. Baker, D. W. Ovenall, J. C. Calabrese, S. A. Westcott, N. J. Taylor, I. D. Williams and T. B. Marder, *J. Am. Chem. Soc.*, 1990, **112**, 9399-9400.
30 H. Braunschweig and M. Colling, *Coord. Chem. Rev.*, 2001, **223**, 1-51.
31 G. Alcaraz and S. Sabo-Etienne, *Coord. Chem. Rev.*, 2008, **252**, 2395-2409.
32 (a) E. Negishi, J. J. Katz and H. C. Brown, *J. Am. Chem. Soc.*, 1972, **94**, 4025-4027; (b) T. E. Cole, R. K. Bakshi, M. Srebnik, B. Singaram and H. C. Brown, *Organometallics*, 1986, **5**, 2303-2307; (c) J. A. Soderquist, K. Matos, C. H. Burgos, C. Lai, J. Vacquer and J. R. Medina, in *Contemporary Boron Chemistry*, eds. M. G. Davidson, A. K. Hughes, T. B. Marder and K. Wade, Royal Society of Chemistry, Cambridge, UK, 2000, pp. 472-482.
33 (a) R. A. Bartlett, H. V. R. Dias, M. M. Olmstead, P. P. Power and K. J. Weese, *Organometallics*, 1990, **9**, 146-150; (b) D. J. Parks, W. E. Piers and G. P. A. Yap, *Organometallics*, 1998, **17**, 5492-5503; (c) C. D. Entwistle, T. B. Marder, P. S. Smith, J. A. K. Howard, M. A. Fox and S. A. Mason, *J. Organomet. Chem.*, 2003, **680**, 165-172; (d) T. Murosaki, S. Kaneda, R. Maruhashi, K. Sadamori, Y. Shoji, K. Tamao, D. Hashizume, N. Hayakawa and T. Matsuo, *Organometallics*, 2016, **35**, 3397-3405.
34 D. Gusev, A. Llamazares, G. Artus, H. Jacobsen and H. Berke, *Organometallics*, 1999, **18**, 75-89.
35 *Multinuclear NMR*, ed. J. Mason, Plenum Press, New York, 1987, pp. 625-629.
36 T. St. Amour and D. Fiat, *Bull. Magn. Reson.*, 1980, **1**, 118-129.
37 (a) K. M. Waltz, X. He, C. Muhoro and J. F. Hartwig, *J. Am. Chem. Soc.*, 1995, **117**, 11357-11358; (b) H. Braunschweig, K. Radacki, F. Seeler and G. R. Whittell, *Organometallics*, 2006, **25**, 4605-4610; (c) J. Bauer, H. Braunschweig, R. D. Dewhurst, K. Kraft and K. Radacki, *Chem. - Eur. J.*, 2012, **18**, 2327-2334.
38 R. Frank, J. Howell, R. Tirfoin, D. Dange, C. Jones, D. M. P. Mingos and S. Aldridge, *J. Am. Chem. Soc.*, 2014, **136**, 15730-15741.
39 R. F. W. Bader, *Atoms in Molecules: A Quantum Theory*, Clarendon Press, Oxford, 1990.
40 C. Perthuisot, M. Fan and W. D. Jones, *Organometallics*, 1992, **11**, 3622-3629.
41 W.-D. Wang, I. A. Guzei and J. H. Espenson, *Organometallics*, 2001, **20**, 148-156.
42 R. H. Morris, *Chem. Rev.*, 2016, **116**, 8588-8654.
43 (a) T. Kruck and A. Engelmann, *Angew. Chem., Int. Ed. Engl.*, 1966, **5**, 836; (b) W. J. Miles, Jr. and R. J. Clark, *Inorg. Chem.*, 1968, **7**, 1801-1806; (c) W. J. Miles, Jr., B. B. Garrett and R. J. Clark, *Inorg. Chem.*, 1969, **8**, 2817-2818; (d) R. A. Head, J. F.

Nixon, G. J. Sharp and R. J. Clark, *J. Chem. Soc., Dalton Trans.*, 1975, 2054-2059.
44 J. E. B. B. J. Burger, in *Experimental Organometallic Chemistry - A Practicum in Synthesis and Characterization*, American Chemical Society, Washington, D.C., 1987, vol. 357, pp. 79-98.
45 A. Pelter, K. Smith and H. Brown, *Borane Reagents*, Academic Press, London, 1988.
46 R. K. Harris, E. D. Becker, S. M. Cabral de Menezes, R. Goodfellow and P. Granger, *Pure Appl. Chem.*, 2001, **73**, 1795-1818.
47 G. M. Sheldrick, *Acta Crystallogr., Sect. A: Found. Crystallogr.*, 2008, **64**, 112-122.
48 G. M. Sheldrick, *Acta Crystallogr., Sect. A: Found. Adv.*, 2015, **71**, 3-8.
49 G. M. Sheldrick, *Acta Crystallogr., Sect. C: Struct. Chem.*, 2015, **71**, 3-8.
50 O. V. Dolomanov, L. J. Bourhis, R. J. Gildea, J. A. K. Howard and H. Puschmann, *J. Appl. Crystallogr.*, 2009, **42**, 339-341.
51 J. Britten and W. Guan, MAX3D, max3d.mcmaster.ca